Revisiting levees in southern Texas using Love-wave multichannel analysis of surface waves with the high-resolution linear Radon transform

Julian Ivanov[1], Richard D. Miller[1], Daniel Feigenbaum[1], Sarah L. C. Morton[1], Shelby L. Peterie[1], and Joseph B. Dunbar[2]

Abstract

Shear-wave velocities were estimated at a levee site by inverting Love waves using the multichannel analysis of surface waves (MASW) method augmented with the high-resolution linear Radon transform (HRLRT). The selected site was one of five levee sites in southern Texas chosen for the evaluation of several seismic data-analysis techniques readily available in 2004. The methods included P- and S-wave refraction tomography, Rayleigh- and Love-wave surface-wave analysis using MASW, and P- and S-wave cross-levee tomography. The results from the 2004 analysis revealed that although the P-wave methods provided reasonable and stable results, the S-wave methods produced surprisingly inconsistent shear-wave velocity V_S estimates and trends compared with previous studies and borehole investigations. In addition, the Rayleigh-wave MASW method was nearly useless within the levee due to the sparsity of high frequencies in fundamental-mode surface waves and complexities associated with inverting higher modes. This prevented any reliable V_S estimates for the levee core. Recent advances in methodology, such as the HRLRT for obtaining higher resolution dispersion-curve images with the MASW method and the use of Love-wave inversion routines specific to Love waves as part of the MASW method, provided the motivation to extend the 2004 original study by using horizontal-component seismic data for characterizing the geologic properties of levees. Contributions from the above-mentioned techniques were instrumental in obtaining V_S estimates from within these levees that were very comparable with the measured borehole samples. A Love-wave approach can be a viable alternative to Rayleigh-wave MASW surveys at sites where complications associated with material or levee geometries inhibit reliable V_S results from Rayleigh waves.

Introduction

Seismic data used in this study were originally acquired as part of a research project designed to evaluate the applicability of several seismic techniques to identify, delineate, and estimate the properties of materials within and beneath levees (Ivanov et al., 2004). The seismic surveys were carried out at five sites located within the Rio Grande River floodplain in the San Juan Quadrangle, Texas, USA (Figure 1). This area of the Lower Rio Grande Valley (LRGV) was selected because it had undergone drying and internal desiccation of soils as a result of 11 years of drought (Dunbar et al., 2007). These soil moisture conditions raised concerns with engineers about the internal levee conditions, impermeable core, and impact of extreme soil conditions on the levees' structural characteristics hidden by a permeable shell.

Because the structural health of a soil matrix is governed by the flow of water and air through its pore spaces, large moisture decreases can affect the soil bearing capacity. In this extreme dewatering case, if the soil surrounding the levee undergoes drying beyond design levels it can become deformed. Thus, the core's resistance to cracking can be compromised and can potentially lead to more destructive and therefore devastating failure during high water stages.

The five sites for the original research project were chosen based on regional airborne and surface geophysical surveys and local borehole data. Key factors in selecting these five sites (Figure 2) were abnormally low electromagnetic (EM) conductivities determined from and consistent between airborne and surface geophysical survey data, abnormally high grout intake while backfilling sampling boreholes, and marked shrinkage and visible cracks in year-old preserved cores. (Miller and Ivanov, 2005).

Old Rio Grande oxbows, natural levees, and terraces within the flood plain of the modern Rio Grande River Valley were a primary source for borrow material used during the construction of the levees designed as flood

[1]Kansas Geological Survey, Lawrence, Kansas, USA. E-mail: jivanov@kgs.ku.edu; rmiller@kgs.ku.edu; d570f573@ku.edu; smorton@kgs.ku.edu; speterie@kgs.ku.edu.

[2]U.S. Army Engineer Research and Development Center, Vicksburg, Mississippi, USA. E-mail: joseph.b.dunbar@usace.army.mil.

Manuscript received by the Editor 23 March 2016; revised manuscript received 13 February 2017; published online 11 April 2017. This paper appears in *Interpretation*, Vol. 5, No. 3 (August 2017); p. T287–T298, 14 FIGS.

http://dx.doi.org/10.1190/INT-2016-0044.1.

control structures. The river's floodplain contains Holocene-age deposits (less than 10,000 years) and deposits of Pleistocene age (between 10,000 and 2 million years old) deposited by the Rio Grande River. The levees are primarily positioned on point bar deposits, formed by the meander of the river across its floodplain. LRGV boring data in the San Juan East area identify the alluvial material as typical point bar deposits containing a fine-grained (silt and clay) top stratum, between 1.5 and 3 m thick, and a much thicker coarse-grained (fine to coarse sand and gravel) substratum that extends to the bedrock surface (Dunbar and Ballard, 2003). Borrow material to build the levees was mined locally from these different depositional settings.

Several surface seismic measurements using state-of-the-practice equipment were made following standard procedures, and acquisition parameters were selected for standard and research-oriented surveys (Miller and Ivanov, 2005). Seismic data were separated by mode and propagation characteristics and then analyzed using the same methods that guided the acquisition. These methods included P and S refraction, P and S traveltime tomography (2D turning ray and 3D straight ray through levee), surface-wave propagation patterns, and surface-wave (Rayleigh- and Love-wave) dispersion-curve analysis (multichannel analysis of surface waves [MASW]).

In 2004, seismic data analysis provided reasonable V_P estimates, but it did not provide reliable V_S results for imaging, characterizing, and investigating the levee cores using either refraction tomography (Figure 3) or MASW methods. Refraction tomography V_S values appeared unrealistically high (Figure 3b), most likely due to P-S mode-converted energy (Xia et al., 2002; Ivanov et al., 2004). Fundamental-mode Rayleigh-wave observations did not capture the range of high frequencies necessary to sample the very shallow part of the subsurface and thus did not provide images from within the levees. Analysis of the transverse horizontal component (i.e., SH) data acquired with SH sources targeting Love waves produced dispersion images with a well-developed and predicted curve geometry between approximately 5 Hz to more than 32 Hz. Other surface-wave

Figure 1. (a) Location of the San Juan Quadrangle, Texas, USA, (b) approximate location of the seismic site marked with a bright white square on a Google Earth image, and (c) the magnified white square Google Earth image.

Figure 2. Google Earth aerial image with GPS locations of the study sites 1, 2, 3, 4, and 5 indicated with thick short white lines and numbers.

(mode) data lacked sufficient high-frequency signal components to sample within the levees limiting their use to dispersion-curve 2D sections. As it turns out, this limitation was due to technological barriers encountered at that time (Ivanov et al., 2004).

The MASW method was originally developed to estimate the near-surface shear-wave velocity distribution from high-frequency (≥ 2 Hz) Rayleigh-wave data (Song et al., 1989; Park et al., 1998; Miller et al., 1999; Xia et al., 1999). Shear-wave velocities estimated by MASW have been reliably and consistently correlated with drill data (Miller et al., 1999; Ismail and Anderson, 2007; Casto et al., 2009; Foti et al., 2011). The MASW method has been applied to a wide range of problems that have included investigations of levee bodies and subgrade (Ivanov et al., 2004, 2006; Takahashi et al., 2014).

A review of established approaches of surface-wave methods (SWM) can be found in Socco et al. (2010). Most developments of the SWM in the past five years have included expanded use of the horizontal component of the Rayleigh wave (Boaga et al., 2013; Ikeda et al., 2015), the simultaneous use of guided waves with multimode surface waves in land and shallow marine environments (Boiero et al., 2013), understanding fault geometry (Ikeda et al., 2013), development of V_S profiles to depths of 100 m or deeper for earthquake-response microzonation (Murvosh et al., 2013), and evaluation at landfill sites (Suto, 2013).

The two recent developments that are most significant to this study are the use of the high-resolution linear Radon transform (HRLRT) for dispersion-curve imaging (Luo et al., 2008) and Love-wave inversion (Xia et al., 2012). It was these two seminal advancements that prompted us to revisit the application of the MASW method for SH data acquired using SH sources for estimating V_S from Love-wave analysis.

Method

The MASW method has three distinct steps, and each step has key requirements and outputs that are integral to subsequent steps. Data acquisition is straightforward and results in a single seismic data record or shot gather. These seismic traces in the shot gather are transformed into a dispersion-curve image, using the phase-shift method (Park et al., 1998) or HRLRT (Luo et al., 2008). This image is used to pick a dispersion-curve trend(s) of the Rayleigh wave, which is then inverted to produce a 1D V_S model (Xia et al., 1999). The $V(z)_S$ profile from each shot gather can be displayed below each shot position to give either a 2D (Miller et al., 1999) or 3D (Miller et al., 2003) estimate of the subsurface $V(x, y, z)_S$ model.

The HRLRT is based on the standard LRT, which is a plane-wave decomposition achieved by applying a linear moveout to data and summing over amplitudes (Yilmaz, 1987) and can be written in matrix form as follows:

$$\mathbf{d} = \mathbf{L}\mathbf{m}, \tag{1}$$

where $\mathbf{L} = e^{i2\pi f p x}$ is the forward LRT operator (in which f is the frequency, p is the slowness, and x is the distance between source and receivers), $\mathbf{d}$ is the data, and $\mathbf{m}$ represents the shot gather in the τ-p domain (Luo et al., 2008), where τ is the zero-offset intercept time. Standard LRT results can then be represented in a matrix form as

$$\mathbf{m}_{\text{adj}} = \mathbf{L}^T\mathbf{d}, \tag{2}$$

where $\mathbf{m}_{\text{adj}}$ denotes a low-resolution Radon panel using the adjoint operator $\mathbf{L}^T$. From equation 2, the inverse operator can be denoted using the preconditioned least-squares operator $\mathbf{L}^{-1}$ for the HRLRT. This development was initially proposed by Thorson and Claerbout (1985) for the hyperbolic Radon transform. It was further developed by using the least-squares approach (Yilmaz, 1989; Sacchi and Ulrych, 1995), improved by weighted preconditioning (Trad et al., 2002), and applied to dispersion-curve imaging (Luo et al., 2008).

The MASW method can be applied to Love waves in a manner similar to that of Rayleigh waves. Love-wave analysis, of course, requires the use of data recorded by transverse horizontal-component receivers and excited by SH sources. For this levee study, the MASW method was applied to transverse polarized shear-wave data acquired at sites where vertically polarized Rayleigh-wave data were acquired and proved inconclusive using standard MASW approaches. The key to the effective application of MASW on Love waves was that the HRLRT transform's created dispersion curves with sufficient

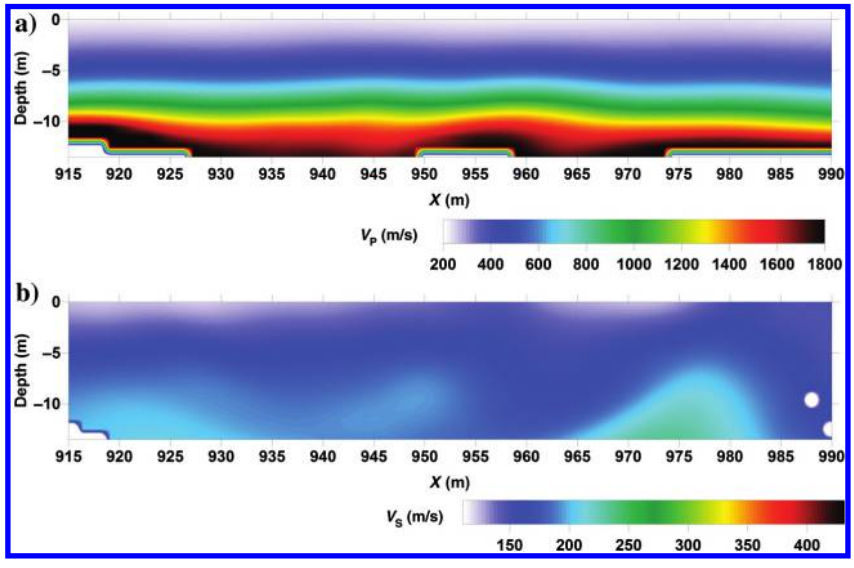

Figure 3. Refraction tomography solutions for the second levee site: (a) P-wave and (b) S-wave.

signal-to-noise ratios that allowed for the effective estimation of $V(z)_S$ profiles.

Data acquisition

A series of seismic investigations were undertaken at five levee sites each with unique mechanical/material properties and all located in the San Juan Quadrangle, Texas, USA (Figure 1). The levees were approximately 5 m high and possessed a one-to-three slope on each side. Each site was in close proximity to locations where boring samples were retrieved and used to correlate and guide the seismic investigations. The series of seismic investigations conducted at all levee sites included one 2D, 2C profile acquired along the crest of the levee and one at the toe of the levee. Receiver station spacing was 0.9 m with two receivers at each location (one 10 Hz compressional-wave geophone and one 14 Hz shear-wave geophone). Shear-wave receivers were oriented to be sensitive to motion perpendicular to the axis of the levee (SH). Sources tested included variously sized sledgehammers and a mechanical weight drop, each impacting striker plates. The total spread length was 108 m with 120 channels recording vertical-component signals and 120 channels recording horizontal-component signals (Figure 4).

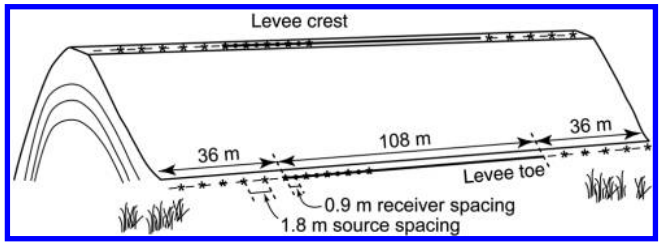

Figure 4. Crest and toe levee seismic data acquisition diagram.

Figure 5. Shear-wave source operated along the crest at site 2.

The sources were optimized based on the mode and the desired energy characteristics. Source spacing through the spread was 1.8 m for sites 1, 2, and 3, and 3.6 m for sites 4 and 5 (Figure 2) with off-end shooting extending a distance equivalent to the maximum depth of investigation. After each profile was acquired using the various impact sources in the compressional-wave orientation, data were acquired a second time using the same sensors and a uniquely designed shear-wave source oriented orthogonally to the levee crest (Figure 5).

Results

Conventional analysis

Having available seismic data that were acquired with multiple sources shot off-end with a fixed extra-long spread length (relative to what would normally be considered an optimal MASW spread size) allowed for efficient and optimal data offset selections for various analysis flows (Miller et al., 2003). The Rayleigh-wave data were evaluated for optimum spread-length and source-offset parameters as deemed ideal for the method at that time. These optimum acquisition geometries were then used to extract from the fixed spread shorter-spread groups emulating a roll-along acquisition pattern.

To maximize the lateral resolution of the processed data, the recording spread used for the calculation of each dispersion curve needs to be as short as possible, while providing an adequate range of frequencies and sufficient quality of the fundamental mode to maximize the picking accuracy of the fundamental-mode dispersion curve. Analysis of several spread sizes demonstrated that shorter spreads, although ideal for resolution, were not sufficient for separating the fundamental mode from the higher modes (Miller and Ivanov, 2005). In general, a 40 channel spread (Figure 6) provided the optimal separation of the fundamental mode from the higher modes.

Near-source offsets were evaluated as part of our efforts to preserve the high-frequency components of the fundamental mode. In spite of these efforts, the fundamental-mode Rayleigh-wave energy collected at the levee sites did not possess the higher frequencies (Figure 7a) necessary to sample the very shallow part of the subsurface, which included the levee core. Higher-mode energy removal using various proven techniques (Park et al., 2002; Ivanov et al., 2005) was successful, to a limited degree, but it unfortunately did not uncover fundamental-mode energy at frequencies above 18 Hz that would characterize the shear-wave velocity inside the levee (Figure 7b). The fundamental-mode dispersion curves were produced using the portion of data exhibiting a high level of coherence in the dispersion curve and that could be selected with high confidence (e.g., approximately 4–11 Hz). These limited spectral data segments were inverted across most of the line to produce a 2D V_S image (Figure 8) that was depth limited but

accurate. The top approximately 8 m were not imaged due to the lack of reliable high frequencies.

Love-wave analysis of the transverse polarized shear-wave data (Figure 9) using a conventional approach to overtone analysis produced encouraging dispersion trends across a frequency range from 5 Hz to more than 32 Hz (Figure 10a). Using a half-wavelength approximation of depth (Rix and Leipski, 1991) on overtone images, it was possible to approximately estimate V_S as shallow as about 1.6 m (e.g., wavelength = velocity/frequency). The phase velocity at 32.5 Hz is around 105 m/s. Thus, the wavelength is $105/32.5 = 3.2$ m, and the depth half of that is $3.2/2 = 1.6$ m, so that it is possible to sample the levees with the shear-wave data. However, very few records possessed data of such high fidelity. A lack of consistency in recorded data resulted in most of the images not possessing a sufficient range of high frequencies to sample the shallow portion of the levees (Figure 10b). Thus, we were limited at the time to dispersion-curve 2D sections that were constrained by the technological limitations at that time (Ivanov et al., 2004).

HRLRT analysis

Shear-wave seismic data from site 2 (Figure 2) possessed the right characteristics to demonstrate the utility of the HRLRT analysis and were therefore reprocessed using SurfSeis (v.5.3), which supports HRLRT imaging and Love-wave modeling and inversion. Initially, we estimated dispersion-curve images (Figure 10) using the conventional phase-shift method (Park et al., 1998). However most of the images did not contain high-frequency components of the fundamental-mode Love wave (Figure 10b) and the inversion failed to provide shallow V_S estimates for the levee (results not shown for brevity).

Previous successes with the HRLRT motivated a series of experiments designed to optimally produce dispersion-curve images from the shear-wave levee data. It was gratifying that for more than 75% of the overtone images, the HRLRT measurably extended the Love-wave

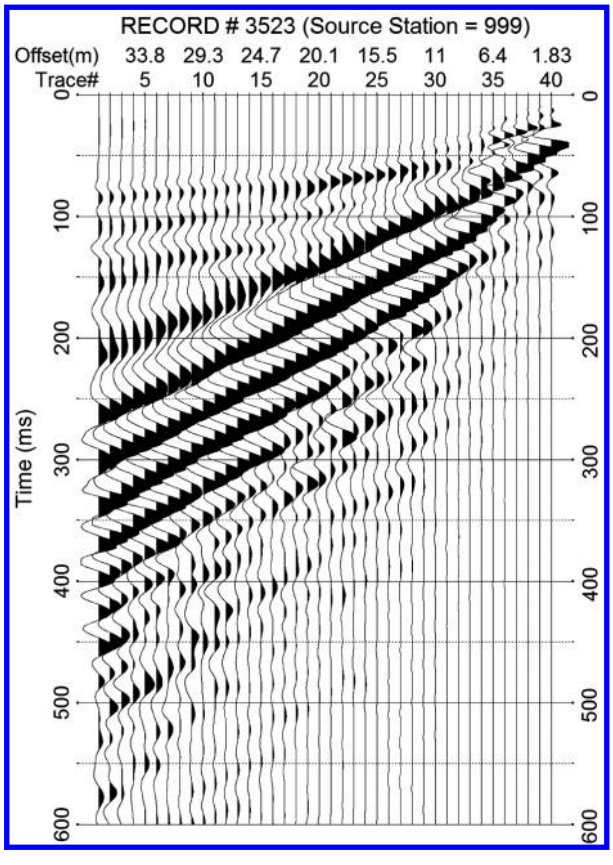

Figure 6. Forty-channel spread vertical-component seismic data, record 3523.

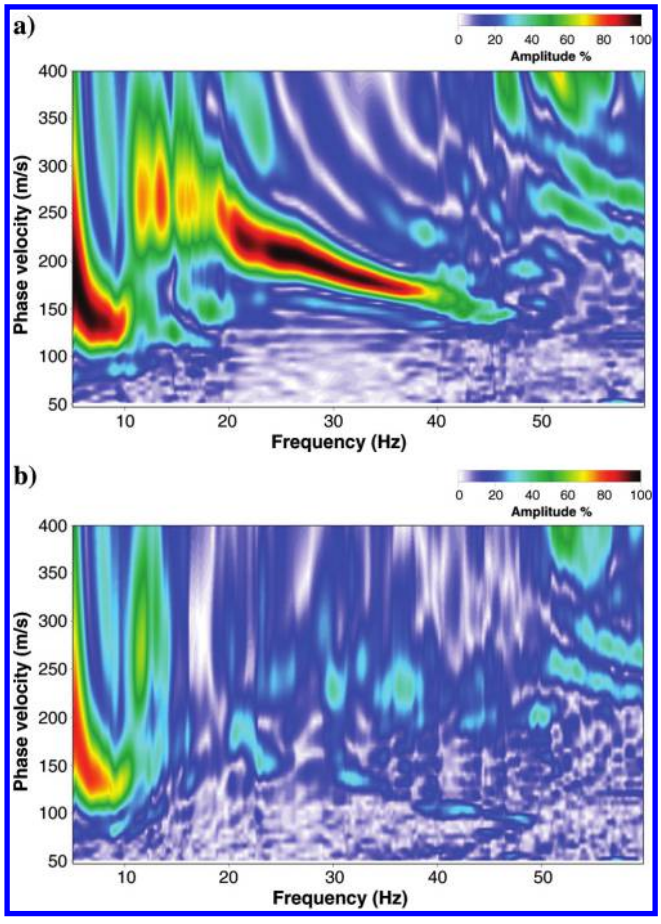

Figure 7. Record 3516 Rayleigh-wave dispersion-curve images in the phase velocity — frequency from a 40 channel (a) raw data and (b) after filtering higher mode energy.

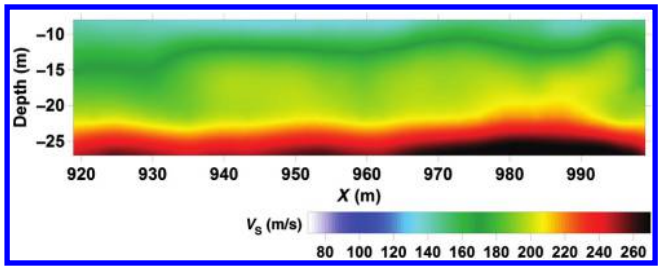

Figure 8. Line 2, Rayleigh-wave MASW V_S.

fundamental-mode frequency range (Figure 11a). For example, the approximately 6–14 Hz interval at 150–120 m/s fundamental-mode energy trend in Figure 10b was extended to include around 14–52 Hz range (Figure 11a). Furthermore, HRLRT helped separate the interfering energy patterns in the 14–20 Hz range.

Encouraged by these results, we shortened the HRLRT spread size in search of the minimal spread length for better lateral resolution, which would still remain large enough to separate the fundamental mode from the higher modes. The critical step was to retain sufficient coherence in the dispersion curve to trace coherent fundamental-mode energy trends. A spread using just the first half of the optimally selected traces seemed reasonable for such a trade-off (Figure 11b). This shorter offset trace selection criteria resulted in a fundamental mode that was less coherent between approximately 5–20 Hz and retained some interference characteristics associated with higher modes but still allowed an interpretable dispersion trend to be estimated.

The 2D V_S image obtained from inverting Love-wave dispersion curves (Figure 12a) was consistent with the geologic expectations. A high-velocity anomaly between 2 and 4 m in depth was apparent across most of the section. This high-velocity interval was consistent and interpreted as the levee core. Probably more significant were the low-velocity anomalies interpreted as the core in the V_S image. The most notable of these anomalies was between approximately 961–966 and 974–979 m along the x-coordinate. Love-wave V_S results complemented V_S results from Rayleigh-wave analysis (Figure 12b). Combining the Rayleigh- and Love-wave V_S tomograms, the missing upper 8 m on the Rayleigh-wave cross section and the reduced penetration of the Love-wave section produces a cross section with a much a wider depth range of V_S estimates.

The distribution and range of velocity anomalies were consistent with the documented variations in material types used during construction and the construction processes itself. It is not clear if velocity information alone is sufficient to identify areas with a high density of cracks (high-permeability zones), which might be a result of the dewatering of the expansive clays during drought, which were used in some places during core construction. However, it is unlikely that reduction in material stiffness within the levee core could be an indicator of a potential risk zone for failure. We interpreted the low-velocity anomalies at 920 m and $2 < z < 4$ m, at 964 m and $2 < z < 3$ m, and at 977 m and $2 < z < 5$ m as possible crack zones in the levee core. The high-velocity anomaly between 5 and 7 m in depth

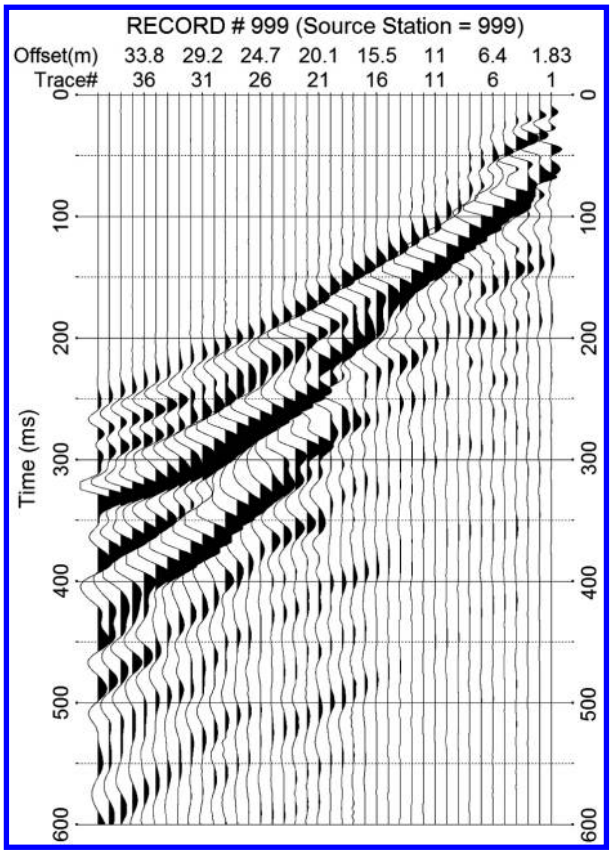

Figure 9. Forty-channel spread transverse horizontal-component seismic data, record 999.

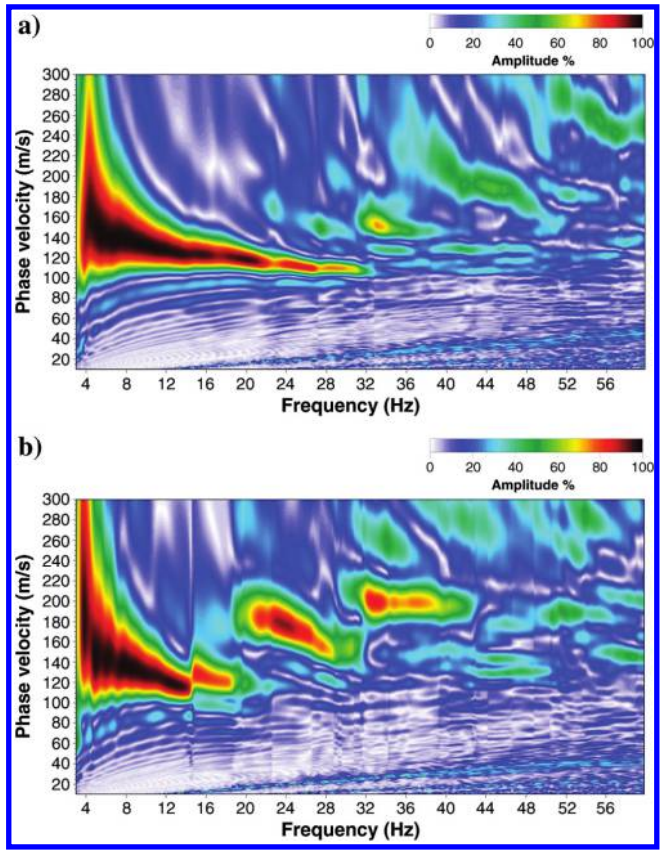

Figure 10. Love-wave dispersion-curve images of different quality from different shot locations: (a) with (record 1077) and (b) without (record 1013) high frequencies of the fundamental mode at about 120 m/s in the range of approximately 20–32 Hz.

at the 977 m offset location is likely the result of clay particles migrating into the levee base. The velocity values at the trench repair location (967–973 m) were consistent with the expected levee condition after the backfill repair.

Multimode inversion with HRLRT

It is evident that the HRLRT dispersion-curve images (Figure 11) provided a better opportunity for identifying higher-mode dispersion trends so that they can be incorporated into the inversion scheme. Benefits from incorporating the higher modes can include a greater investigation depth, improved inversion stability, and higher vertical resolution (Xia et al., 2003; Luo et al., 2007). However, efforts to include higher-mode dispersion-curve trends proved challenging for these Love-wave data. Higher-mode trends varied rapidly from one record to another and represented a daunting challenge to interpret. It can be hypothesized that in the presence of greater lateral variability, the dispersion-curve image can include more than one set of fundamental-mode and higher trends. Each of these sets could represent a different velocity-model encompassed by the seismic spread. In such cases, more than one fundamental mode can be present and be easily mistaken for a higher mode. Similar misidentification can occur with higher modes. Consequently, several equally possible inversion V_S results can be obtained that are numerically quite different.

To resolve such ambiguities, we adopted a unique approach for improving confidence in interpreting modes in the dispersion-curve images. Using the 1D V_S model, estimated from inverting the most likely fundamental mode energy, the dispersion curves of the fundamental and first five higher modes were calculated. Thus, the theoretical locations of the higher modes could be established as a guide. Higher-mode patterns will be consistent with various interpretations of the fundamental mode trend. This approach helps to optimize the interpretation of fundamental mode energy throughout the usable frequency band and refines the search for expected locations of higher-mode energies in the dispersion-curve image. For this reason, the theoretical dispersion curves for these six modes were plotted on the corresponding overtone image.

Points of the calculated higher modes that appear in the vicinity of a velocity trend are interpreted as being representative of the corresponding higher mode. That trend is then identified as the corresponding modeled mode and included in the multimode inversion. This approach was applied to the images that were of sufficient quality to make these assignments. For approximately two-thirds of the images, two modes (fundamental and the first higher mode) were identified with confidence, and for approximately one-third of the images, three modes (fundamental and the first two higher mode) were estimated. Each multimode dispersion curve was instrumental in obtaining higher resolution results (i.e., using a 20-layer model) with 1D V_S inversion, which were ultimately assembled into a 2D V_S section (Figure 13).

The model points of the fundamental and first higher mode (yellow and red circles) fall on observed energy trends, whereas the calculated second through fifth

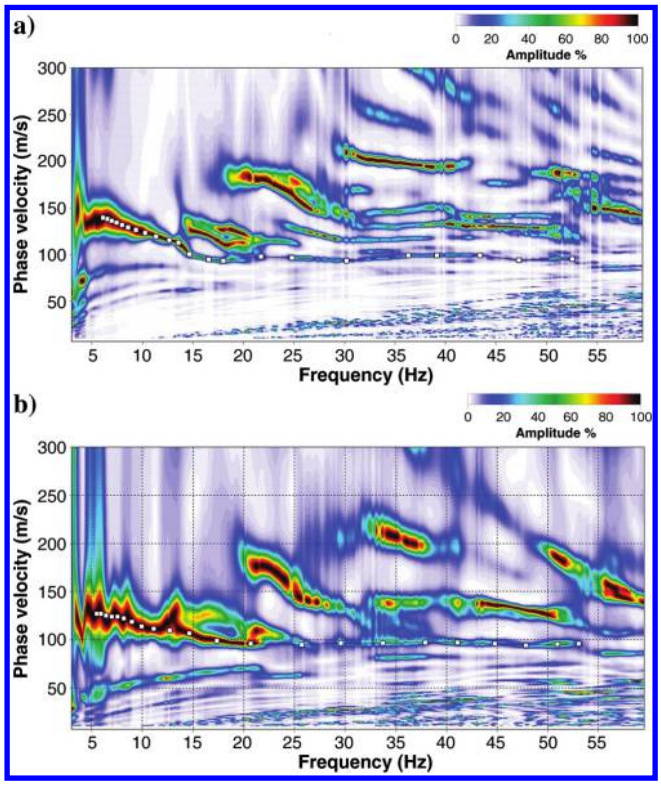

Figure 11. Love-wave dispersion-curve images of record 1013 having fundamental mode high frequencies when using the HRLRT with (a) identical spread size and (b) half the spread size. Some of the dispersion curve picks between 20 and 52 Hz are intentionally in-between fundamental mode energy for visualization purposes.

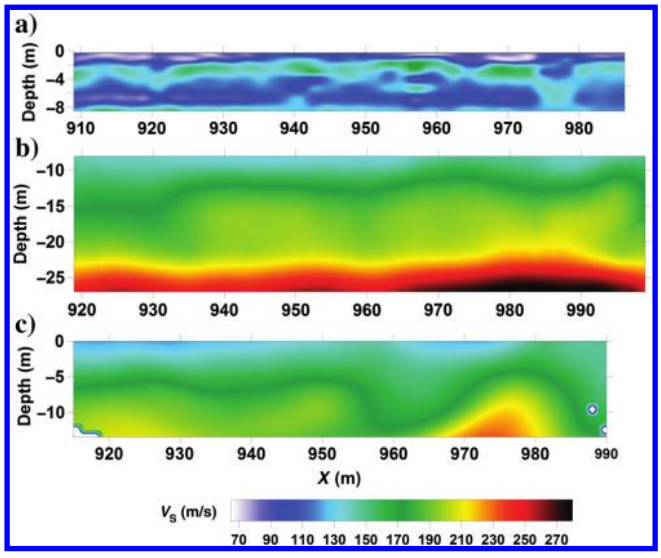

Figure 12. Shear-wave data V_S estimates from (a) Love-wave inversion, (b) Rayleigh-wave inversion, and (c) shear-wave refraction tomography.

higher modes are a poor match to any of the remaining dispersion-curve energy trends (Figure 14a). It is reasonable to suggest that these remaining features are related to heterogeneity (i.e., from another velocity model). Applying the same process to the next record, 1015, the calculated fundamental and next three higher modes correlated quite well with dispersion-curve trends on overtone analysis images. Similar coherent energy features corresponding to the forward-model-calculated second and third higher modes of record 1015 were observed on record 1013. However, these higher mode patterns were not consistent with the higher modes depicted in the forward model calculated from the actual fundamental mode of record 1013. Considering that approximately 75% of the seismic spread of these two records overlapped, it is hypothesized that higher mode energy unique to record 1013 seismic spread was dominated by energies from traces contributing only to the velocity model representative of record 1015.

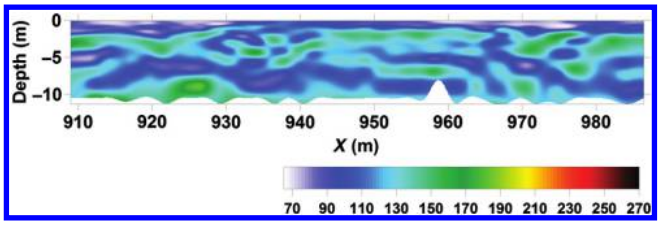

Figure 13. Shear-wave data V_S estimates from Love-wave multimode inversion.

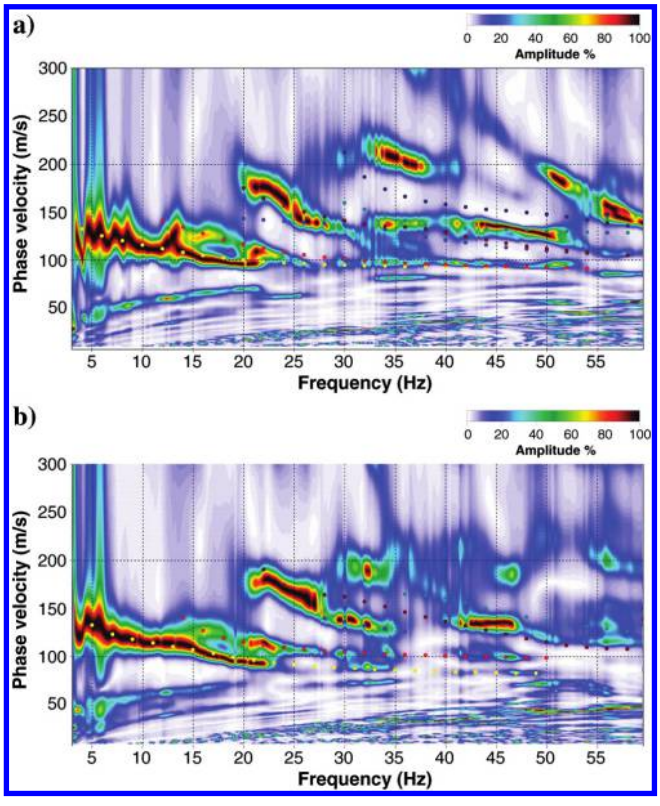

Figure 14. Calculated fundamental (yellow circles) and the first five higher modes (red, blue, brown, green, and black circles accordingly) of two consecutive records (a) 1013 and (b) 1015.

The 2D V_S image that is the product of multimode inversion (Figure 13) provided greater maximum imaging depth (approximately 10 versus 8 m) and vertical resolution (20 versus 10 layers) compared with the fundamental-mode only 2D V_S image (Figure 12a). The multimodal-based V_S image supports the previous interpretation of low-velocity anomalies at 940, 964, and 977 m and suggests an indication of another anomaly with alternating low- and high-velocity values at 932–936 m for $2 < z < 5$ m.

Discussion

The V_S profiles inverted from Love waves support our 2004 hypothesis that apparent shear-wave refraction (first) arrivals were being influenced by P- to S-wave mode conversions leading to higher than expected 2D V_S estimates from refraction tomography (Figure 12c). Love-wave research has shown that fundamental and first higher mode Love-wave dispersive energy can possess uniform, uncluttered trends, and much simpler shapes (Xia et al., 2012) than Rayleigh-wave dispersion images. Seismic data recorded during this study demonstrate that Love-wave energy fields can lack high-frequency fundamental-mode energy (consistent with Rayleigh waves). This is contrary to our experience with synthetic and real-world data that Love-wave fundamental modes generally span a wide and more complete frequency range relative to the Rayleigh-wave modes.

The scale of lateral variability in the 2D V_S results appears smaller than the dominant wavelength thus violating the general MASW method assumption of horizontally layered medium (also known as local layered medium approximation) used for dispersion-curve calculations and inversion (Xia et al., 1999; Luo et al., 2007). Currently, it is unclear to what extent such violations affect the accuracy of the final V_S estimates, but awareness of potential errors as a result of such violations seems appropriate. Further research involving synthetic seismic-data modeling (Zeng et al., 2012a) can clarify the limitations of the 1D assumption.

The levee shape can be another source of errors. Using 3D numerical models, Min and Kim (2006) showed that the levee shape can cause some Rayleigh-wave fundamental-mode phase-velocity overestimations. Likewise, Zeng et al. (2012b) demonstrated that the Rayleigh-wave dispersion-curve image can be contaminated by energies associated with the levee shape. The same study also showed that if the distance of the seismic line from the levee edge is >2 m, then the effects of the levee shape on the estimation of the fundamental and the first higher-mode energies can be nearly negligible. Assuming that the impact of the levee shape on the Love wave is similar to that of the Rayleigh wave, seismic data for these levees lines were acquired at least 2 m from the levee edge (Figure 5). Furthermore, our multimode picking approach (mentioned earlier)

helped us avoid sporadic energies associated with the levee shape.

From the dispersion data displayed here, HRLRT images can be void of fundamental mode Love-wave energy in a narrow frequency (e.g., approximately 3–6 Hz) range (Figure 11). A variety of techniques could be developed to correct this situation. Recovering those very low frequency energies was not a focus of this study because the longer wavelengths are significant when imaging deeper parts of the section where, in our case, we were able to use the Rayleigh-wave approach effectively.

Reprocessing vertical-component data with the HRLRT for use in MASW analysis did not help enhance fundamental-mode Rayleigh waves at frequencies above approximately 20 Hz (images not shown for brevity). This finding is consistent with the conventional dispersion-curve imaging study in 2004. We hypothesize that higher frequency fundamental-mode Rayleigh-wave energy was not observed due to the purely horizontally orientation of the recorded energy; i.e., it lacked a vertical component. Such a phenomenon was noted for low-frequency models in which a high-velocity contrast was encountered (Boaga et al., 2013). We speculate that this effect could be observed for a range of models including the Brownsville levees. Further research and model studies could clarify if this was possible for our velocity models.

Multimode dispersion-curve patterns rapidly varied in shape and intensity from one record to another at this levee site and were difficult to interpret. Higher mode dispersion-curve trends could only be reasonably interpreted after using HRLRT imaging in conjunction with event identification through multimode dispersion-curve modeling based on fundamental-mode-only inversion results.

Conclusion

Obtaining reasonable V_S estimates within the LRGV levees from surface seismic data was only possible with the incorporation of HRLRT (for dispersion curve imaging) and Love-wave inversion applied to horizontally polarized surface wave data acquired along the crest of the levees in 2004. This approach should be effective for estimating V_S properties at other levee sites where it is difficult to estimate the higher order Rayleigh-wave modes. Our study demonstrates that HRLRT can be an effective means of increasing the lateral resolution of the MASW method. The method produces high-fidelity dispersion-curve images with significantly shorter (up to 50% reduce) receiver spread lengths in comparison with the more commonly used method to produce overtone images. This approach significantly enhances the potential of MASW to locate V_S (i.e., material stiffness) anomalies substantially smaller than a wavelength. This improved resolution dramatically increases the opportunities to include the Love-wave MASW method with more common geophysical tools used for assessing areas with failure risk in levees.

Acknowledgments

Support and assistance from U.S. IBWC is greatly appreciated and without which this research would not have been possible. The SurfSeis (v.5.3) software used in this paper was developed by the Kansas Geological Survey. The U.S. Border Patrol provided a safe working environment for our field crew. We also appreciate M. Brohammer for her assistance in manuscript preparation. G. Schuster, N. Nakata, and three anonymous reviewers helped improve the manuscript. Permission to publish this paper was granted by the commissioner of the U.S. Section of the International Boundary and Water Commission, and by the director of the Geosciences and Structures Laboratory, ERDC.

References

Boaga, J., G. Cassiani, C. L. Strobbia, and G. Vignoli, 2013, Mode misidentification in Rayleigh waves: Ellipticity as a cause and a cure: Geophysics, **78**, no. 4, En17–En28, doi: 10.1190/geo2012-0194.1.

Boiero, D., E. Wiarda, and P. Vermeer, 2013, Surface- and guided-wave inversion for near-surface modeling in land and shallow marine seismic data: The Leading Edge, **32**, 638–646, doi: 10.1190/tle32060638.1.

Casto, D. W., B. Luke, C. Calderon-Macias, and R. Kaufmann, 2009, Interpreting surface-wave data for a site with shallow bedrock: Journal of Environmental and Engineering Geophysics, **14**, 115–127, doi: 10.2113/JEEG14.3.115.

Dunbar, J. B., and R. F. Ballard, 2003, Trip report: Levee trench study, Retamal Levee, San Juan, TX: U.S. Army Engineer Research and Development Center.

Dunbar, J. B., J. L. Llopis, G. L. Sills, E. W. Smith, R. D. Miller, J. Ivanov, and R. F. Corwin, 2007, Conditional Assessment of Levees, U.S. Section of the International Boundary and Water Commission; Report 5, Flood Simulation Study of Retamal Levee, Lower Rio Grande River, Tx: Technical Report ERDC TR-03-4, US Army Engineer Research and Development Center.

Foti, S., S. Parolai, D. Albarello, and M. Picozzi, 2011, Application of surface-wave methods for seismic site characterization: Surveys in Geophysics, **32**, 777–825, doi: 10.1007/s10712-011-9134-2.

Ikeda, T., T. Matsuoka, T. Tsuji, and T. Nakayama, 2015, Characteristics of the horizontal component of Rayleigh waves in multimode analysis of surface waves: Geophysics, **80**, no. 1, EN1–EN11, doi: 10.1190/geo2014-0018.1.

Ikeda, T., T. Tsuji, and T. Matsuoka, 2013, Window-controlled CMP crosscorrelation analysis for surface waves in laterally heterogeneous media: Geophysics, **78**, no. 6, En95–En105, doi: 10.1190/geo2013-0010.1.

Ismail, A., and N. Anderson, 2007, Near-surface characterization of a geotechnical site in north–east Missouri using shear-wave velocity measurements: Near Surface Geophysics, **5**, 331–336, doi: 10.3997/1873-0604.2007014.

Ivanov, J., R. D. Miller, R. F. Ballard, J. B. Dunbar, and J. Stefanov, 2004, Interrogating levees using seismic meth-

ods in southern Texas: 74th Annual International Meeting, SEG, Expanded Abstracts, 1413–1416.
Ivanov, J., R. D. Miller, N. Stimac, R. F. Ballard, J. B. Dunbar, and S. Smullen, 2006, Time-lapse seismic study of levees in southern New Mexico: 76th Annual International Meeting, SEG, Expanded Abstracts, 3255–3259.
Ivanov, J., C. B. Park, R. D. Miller, and J. H. Xia, 2005, Analyzing and filtering surface-wave energy by muting shot gathers: Journal of Environmental and Engineering Geophysics, **10**, 307–322, doi: 10.2113/JEEG10.3.307.
Luo, Y., J. Xia, J. Liu, Q. Liu, and S. Xu, 2007, Joint inversion of high-frequency surface waves with fundamental and higher modes: Journal of Applied Geophysics, **62**, 375–384, doi: 10.1016/j.jappgeo.2007.02.004.
Luo, Y. H., J. H. Xia, R. D. Miller, Y. X. Xu, J. P. Liu, and Q. S. Liu, 2008, Rayleigh-wave dispersive energy imaging using a high-resolution linear Radon transform: Pure and Applied Geophysics, **165**, 903–922, doi: 10.1007/s00024-008-0338-4.
Miller, R. D., T. S. Anderson, J. Ivanov, J. C. Davis, R. Olea, C. Park, D. W. Steeples, M. L. Moran, and J. Xia, 2003, 3-D characterization of seismic properties at the smart weapons test range, YPG: 73rd Annual International Meeting, SEG, Expanded Abstracts, 1195–1198.
Miller, R. D., and J. Ivanov, 2005, Seismic Tests on IBWC Levees: Weslaco: Kansas Geological Survey, Open-file Report, 56.
Miller, R. D., J. Xia, C. B. Park, and J. M. Ivanov, 1999, Multichannel analysis of surface waves to map bedrock: The Leading Edge, **18**, 1392–1396, doi: 10.1190/1.1438226.
Min, D.-J., and H.-S. Kim, 2006, Feasibility of the surface-wave method for the assessment of physical properties of a dam using numerical analysis: Journal of Applied Geophysics, **59**, 236–243, doi: 10.1016/j.jappgeo.2005.09.004.
Murvosh, H., B. Luke, and C. Calderon-Macias, 2013, Shallow-to-deep shear wave velocity profiling by surface waves in complex ground for enhanced seismic microzonation of Las Vegas, Nevada: Soil Dynamics and Earthquake Engineering, **44**, 168–182, doi: 10.1016/j.soildyn.2012.09.002.
Park, C. B., R. D. Miller, and J. Ivanov, 2002, Filtering surface waves: 72nd Annual International Meeting, SEG, Expanded Abstracts, 1228–1230.
Park, C. B., R. D. Miller, and J. Xia, 1998, Imaging dispersion curves of surface waves on multi-channel record: 68th Annual International Meeting, SEG, Expanded Abstracts, 1377–1380.
Rix, G. J., and A. E. Leipski, 1991, Accuracy accuracy and resolution of surface wave inversion, *in* S. K. Bhatia and G. W. Blaney, eds., Proceedings of Sessions Sponsored by the Geotechnical Engineering: (Geotechnical special publication) American Society of Civil Engineers, 17–23.
Sacchi, M. D., and T. J. Ulrych, 1995, High-resolution velocity gathers and offset space reconstruction: Geophysics, **60**, 1169–1177, doi: 10.1190/1.1443845.
Socco, L. V., S. Foti, and D. Boiero, 2010, Surface-wave analysis for building near-surface velocity models: Established approaches and new perspectives: Geophysics, **75**, no. 5, 75A83–75A102, doi: 10.1190/1.3479491.
Song, Y. Y., J. P. Castagna, R. A. Black, and R. W. Knapp, 1989, Sensitivity of near-surface shear-wave velocity determination from Rayleigh and love waves: 59th Annual International Meeting, SEG, Expanded Abstracts, 509–512.
Suto, K., 2013, MASW surveys in landfill sites in Australia: The Leading Edge, **32**, 674–678, doi: 10.1190/tle32060674.1.
Takahashi, T., T. Aizawa, K. Murata, H. Nishio, and T. Matsuoka, 2014, Soil permeability profiling on a river embankment using integrated geophysical data: 84th Annual International Meeting, SEG, Expanded Abstracts, 4534–4538.
Thorson, J. R., and J. F. Claerbout, 1985, Velocity-stack and slant-stack stochastic inversion: Geophysics, **50**, 2727–2741, doi: 10.1190/1.1441893.
Trad, D. O., T. J. Ulrych, and M. D. Sacchi, 2002, Accurate interpolation with high-resolution time-variant Radon transforms: Geophysics, **67**, 644–656, doi: 10.1190/1.1468626.
Xia, J. H., R. D. Miller, and C. B. Park, 1999, Estimation of near-surface shear-wave velocity by inversion of Rayleigh waves: Geophysics, **64**, 691–700, doi: 10.1190/1.1444578.
Xia, J. H., R. D. Miller, C. B. Park, and G. Tian, 2003, Inversion of high frequency surface waves with fundamental and higher modes: Journal of Applied Geophysics, **52**, 45–57, doi: 10.1016/S0926-9851(02)00239-2.
Xia, J. H., R. D. Miller, C. B. Park, E. Wightman, and R. Nigbor, 2002, A pitfall in shallow shear-wave refraction surveying: Journal of Applied Geophysics, **51**, 1–9, doi: 10.1016/S0926-9851(02)00197-0.
Xia, J. H., Y. X. Xu, Y. H. Luo, R. D. Miller, R. Cakir, and C. Zeng, 2012, Advantages of using multichannel analysis of love waves (MALW) to estimate near-surface shear-wave velocity: Surveys in Geophysics, **33**, 841–860, doi: 10.1007/s10712-012-9174-2.
Yilmaz, O., 1987, Noise and multiple attenuation, *in* Seismic data analysis: SEG investigations in Geophysics 10, 837–1000.
Yilmaz, O., 1989, Velocity-stack processing: Geophysical Prospecting, **37**, 357–382, doi: 10.1111/j.1365-2478.1989.tb02211.x.
Zeng, C., J. H. Xia, R. D. Miller, and G. P. Tsoflias, 2012a, An improved vacuum formulation for 2D finite-difference modeling of Rayleigh waves including surface topography and internal discontinuities: Geophysics, **77**, no. 1, T1–T9, doi: 10.1190/geo2011-0067.1.
Zeng, C., J. H. Xia, R. D. Miller, G. P. Tsoflias, and Z. J. Wang, 2012b, Numerical investigation of MASW applications in presence of surface topography: Journal of Applied Geophysics, **84**, 52–60, doi: 10.1016/j.jappgeo.2012.06.004.

Julian Ivanov received an M.S. engineering (1987) in geophysics from the Higher Institute of Mining and Geology "St. Ivan Rilsky," Sofia, and a Ph.D. (2002) in geology with an emphasis in geophysics from the University of Kansas. He gained experience in different branches of geophysics working for Geology & Geophysics Co., Geocom, and Schlumberger. He is an assistant research professor at the Kansas Geological Survey. He has taught more than 60 two-day short courses and workshops on the MASW method. His research interests include the characterization of near-surface materials with applications to engineering and environmental problems by using seismic geophysical methods. He is particularly drawn to forward modeling, nonuniqueness, and inversion of first arrivals (i.e., refraction/tomography), surface waves, full-waveform inversion, inversion with other geophysical methods, and in general. His inversion research is exploring the use of a priori information for reducing/minimizing inversion nonuniqueness and obtaining as accurate as possible inversion results. His focus is on the development and application of seismic refraction/tomography and surface-wave analysis techniques. He is also involved in software development for making such techniques available to the geophysical public functioning as a scientist, software engineer, programmer, project and quality-assurance manager, and a user experience designer. He is a member of SEG, EEGS, and EAGS.

Richard D. Miller (Rick) received a B.A. in physics from Benedictine College, an M.S. in physics (emphasis geophysics) from the University of Kansas (KU), and a Ph.D. in geophysics from the University of Leoben, Austria. He is a senior scientist at the Kansas Geological Survey (KGS), a research and service division of KU. He also holds a courtesy appointment as associate professor of geology at KU. He has been at the KGS since 1983. He has published more than 90 peer-reviewed journal papers and a half-dozen book chapters. His scientific interests focus on the application of shallow, high-resolution seismic methods to a wide assortment of problems ranging from energy to engineering to the environment.

Daniel Z. Feigenbaum received a B.S. (2014) in geology with a concentration in geophysics from the University of Kansas, where he is also pursuing an M.S. in geology with a concentration in geophysics. He is a graduate research assistant at the Kansas Geological Survey. His research primarily focuses on seismic reflection data processing with an emphasis on migration velocity analysis. He also concentrates on long wavelength static corrections through the implementation of first-arrival tomography, using optimal reference models, to produce more accurate seismic reflection images. In addition to his main areas of focus, he also researches MASW techniques to produce accurate V_S sections of the near surface. He has also worked on research that focused on using filtered MASW data to more precisely calculate attenuation in the near surface, which produced more accurate quality (Q) values for the near surface.

Sarah L. C. Morton received a B.S. (2011) in geoscience from the University of Connecticut and an M.S. (2014) in civil engineering from the University of Connecticut, where she investigated the feasibility of using surface and borehole seismic techniques for mapping surficial materials and depth to bedrock in relation to liquefaction potential and seismic hazard. She completed this work as a U.S. Geological Survey Pathways Intern with the Office of Groundwater, Branch of Geophysics in Storrs, CT. She is a third-year doctoral student in geotechnical engineering at the University of Kansas and a graduate research assistant with the Kansas Geological Survey, Exploration Services. She specializes in the use of surface-wave seismic methods for imaging shallow soil structures local to engineering project sites and tunnel detection. More specifically, she is working on combining geotechnical laboratory methods with seismic imaging techniques to better understand the development and migration of voids that could lead to ground failure. She currently serves as the student program lead of the SEG Near-Surface Technical Section, student representative of the AGU Near-Surface Geophysics Focus Group Executive Committee, and past president of the Association for Women Geoscientists, Osage chapter.

Shelby Peterie received a B.S. (2005) in physics from Benedictine College and an M.S. (2008) in geology with a geophysics emphasis from the University of Kansas. While at the University of Kansas, she investigated variable source coupling and implications for near-surface time-lapse seismology. Since 2008, she has worked at the Kansas Geological Survey as a research geophysicist. She has a broad range of research experience, including diffraction imaging, MASW, vertical seismic profiling, refraction tomography, and earthquake seismology. Her primary research interests include active seismic methods with application to shallow void detection (especially near-surface diffraction imaging) and injection-induced seismicity. She currently oversees the Kansas seismic monitoring network for detecting and locating earthquakes in Kansas.

Joseph Dunbar is a senior research geologist with the U.S. Army Engineer Research and Development Center (ERDC), Geotechnical and Structures Laboratory. He has 38 years of professional experience as an engineering geologist, conducting civil and military studies for the U.S. Army Corps of Engineers (USACE). His career involves several long-term comprehensive geologic and geomorphic mapping studies of floodplains in the Lower Mississippi Alluvial Valley, the Louisiana Deltaic Plain, the LRGV, and the Upper Chesapeake Bay. His work experience has involved geologic, geophysical, and earthquake

hazard studies for USACE levees and dams, and hydrogeologic studies at military ordnance facilities. He was the senior geologist with the Corp's Interagency Performance Evaluation Team, studying the causes of levee and floodwall failures in the greater New Orleans area by Hurricane Katrina. He is a registered geologist in Alabama, Indiana, Louisiana, and Mississippi. He has degrees from Lake Superior State University, the University of Mississippi, and the University of Delaware. He developed the internationally recognized website for downloading USACE-published engineering geology maps of the Lower Mississippi Valley (see lmvmapping.erdc.usace.army.mil) and has authored and coauthored numerous ERDC technical reports and professional journal papers.